Off-axis nulling transfer function measurement: a first assessment

G. Dalla Vedova[1], J.-L. Menut[1], F. Millour[1], R. Petrov[1], F. Cassaing[2], W. C. Danchi[3], S. Jacquinod[4], E. Lhome[5], B. Lopez[1], J. Lozi[6], A. Marcotto[1], J. Parisot[4], J.-M. Reess[4]

[1] *Laboratoire LAGRANGE, Université de Nice-Sophia Antipolis, OCA, 06108 Nice, France,* [2] *ONERA, F-92322 Châtillon, France,* [3] *NASA Goddard Space Flight Center, Greenbelt, MD 20771, USA,* [4] *LESIA, Observatoire de Paris, 5 Place J. Janssen, 92195 Meudon, France,* [5] *ING, Apartado de correos 321 E-38700 Santa Cruz de la Palma, Canary Islands, Spain,* [6] *The University of Arizona, 1077 N Highland, Tucson Arizona 85721, USA*

Abstract. We want to study a polychromatic inverse problem method with nulling interferometers to obtain information on the structures of the exozodiacal light. For this reason, during the first semester of 2013, thanks to the support of the consortium PERSEE, we launched a campaign of laboratory measurements with the nulling interferometric test bench PERSEE, operating with 9 spectral channels between J and K bands. Our objective is to characterise the transfer function, i.e. the map of the null as a function of wavelength for an off-axis source, the null being optimised on the central source or on the source photocenter. We were able to reach on-axis null depths better than 10^{-4}. This work is part of a broader project aiming at creating a simulator of a nulling interferometer in which typical noises of a real instrument are introduced. We present here our first results.

1. Introduction

The observation and the characterisation of dusty debris disks, extrasolar planets, and planetary systems around stars is one of the major astronomical challenge of the 21st century. Direct detection, model fitting, and ultimately imaging of these objects require instruments with very high dynamic range and high angular resolution in order to comply the combination of two major physical constraints. First, there is large flux ratio between the star and the planet or the circumstellar disk, typically $\sim 10^{10}$ in the visible, and $\sim 10^7$ in the infrared. Second, the angular separation between a host star and exoplanet in the habitable zone is typically small. For example, the system Earth-Sun at maximum elongation at the distance of 10 pc has an angular separation of the order of 100 mas or 0.5 μrad which needs an interferometer with a baseline of 20 m at 10 μm.

Currently, there is a large effort to develop concepts able to detect and characterise Earth-like planets (Quirrenbach 2001). In this context, nulling interferometry could play a key role (Bracewell & MacPhie 1979). In last decades, nulling

interferometry has been one of the most studied techniques (Angel & Woolf 1997; Léger et al. 1996a) and these studies led to consider two major projects named DARWIN (Léger et al. 1996b) and TPF-I (Lawson et al. 2007). The goal of these two missions is to detect Earth-like planets into the habitable region and characterise their spectra with eventually markers of the possible presence of life (Danchi et al. 2003). As these instruments are extremely demanding for technical and operational requirements, some intermediate class projects, such as PEGASE (Ollivier et al. 2009) and FKSI (Danchi & Lopez 2007) have been considered. The initial specification was to ensure the exozodiacal light with an accuracy of 1 zodi, i.e. the intensity for a system identical to the solar system, for all Darwin potential targets in order to assess Darwin observations feasibility and priority. Later, it has been understood that this type of M-class space interferometer can have remarkable possibilities to characterise the structures of protoplanetary and debris disks with various signatures of planet presence or formation. A demonstrator PERSEE, acronym of Pegase Experiment for Research and Stabilisation of Extreme Extinction, has been designed and built by a consortium led by CNES and including IAS, LESIA, ONERA, OCA and Thales Alenia Space in order to assess the potential and limits of PEGASE, and lately FKSI.

There is a growing interest in the image reconstruction from interferometric observations, due to the possibility to visualise unsuspected structures and details of the object of interest. Both in model fitting and image reconstruction, the knowledge and the characterisation of the transfer function and the covariance matrix of residuals of the interferometer are critical information, both to optimise the problem inversion and to characterise the quality of the result (Tallon-Bosc 2007; Thiébaut 2009). As a consequence, characterising the off-axis transfer function of a nulling interferometer is of prime interest.

Early in 2013, we started a measurement campaign with the aim of characterising the transfer function with a real nulling interferometer operating in 9 spectral channels in a large spectral band of the infrared. We used the PERSEE test bench to record transmission maps, simulating angularly offset sources with different ranges of baselines and tilts. We obtained a database of measured multiwavelength transmission maps of a nulling interferometer, and are comparing it with its analytical model (section 3.).

2.   Measurement campaign

PERSEE is a fibered nulling interferometer demonstrator built with the aim to achieve a stabilised nulling ratio better than 10^{-4} in a large spectrum range between bands J and K. Lozi et al. (2013) have demonstrated that a polychromatic nulling depth of 10^{-6} with a stability of 10^{-7} could be reached over 10 hours simulating conditions of typical perturbations of a spacecraft such as PEGASE. The detailed optical layout made by Thales Alenia Space is recalled in Table 2. and in Fig.1. The bench is equipped with a fringe sensor (FS) based on the ABCD modulation technique (Shao et al. 1988) and a tip-tilt sensor (FRAS) in order to correct respectively internal OPD between the interferometer arms and tilt errors in closed loop. After the combining stage, a Modified Mach-Zehnder (MMZ) (Jacquinod et al. 2008), dichroic plates separate the various spectral channels and direct them in the appropriate detection chains. The H and K channel signals reach, via a single mode fiber, the nitrogen cooled infrared detector. On the

Table 1.: *Optical components of PERSEE*

M1	45 deg. mirror
M4-M5	nulling periscope
M6	tip-tilt injection
M7-M8	delay line (cat's eye)
M11	FRAS mirror
M9	30 deg. mirror (MMZ)
L3-L4	separating plates (MMZ)
D2	fringe sensor dichroic
M10	off-axis parabola
I	output of MMZ corresponding to the channel A
II	output of MMZ corresponding to the channel B
III	output of MMZ corresponding to the channel D
IV	output of MMZ corresponding to the channel C

IR camera, we have simultaneously polychromatic measurements in 9 channels from $1.65\mu m$ to 2.45 μm. In order to simulate an off-axis source, we introduced on mirrors of PERSEE (M6) a set of commands to drive a displacement in tip-tilt (α, β) and OPD δ. These tip-tilt and OPD can be associated with a simulated baseline B by the relationship $\delta = B \cdot \sin(\alpha)$, where α and β correspond to an angular position on sky relative to the optical axis of the instrument. With commands injected on mirrors M6, we scanned a near-field close to the axis within an angular separation of two Airy disk diameters, defined by the resolution of the considered pupils. We simultaneously measured the flux on the dark output of the MMZ recombiner (III output or channel D, see Table 2.), and a flux reference for the source fluctuations directly at the output of the collimator (see Fig.1). A measurement corresponds to a scan of a grid of points in the near-field off-axis with a fixed baseline and, for each position (α, β, δ), we recorded 20 frames in 0.2 seconds with the IR camera. We make α and δ proportional to each other in order to simulate the variation of the transfer function along a 2-telescope baseline. We also measured the photometry of both arms of the interferometer. We normalised the science channels with fluctuations of the source and we evaluated the photometry in both arms I_A, I_B, and the recombination of both beams of light I_D. We define the measured normalised transfer function $\bar{T}^B(\alpha, \beta)$ (Eq.1), and the theoretical transfer function of PERSEE, given in Hénault et al. (2011).

$$\bar{T}^B_{\text{meas}}(\alpha, \beta) = \frac{I_D(\alpha, \beta, \delta)}{I_A(\alpha, \beta, \delta) + I_B(\alpha, \beta, \delta) + 2\sqrt{I_A(\alpha, \beta, \delta)I_B(\alpha, \beta, \delta)}} \quad (1)$$

$$T^B_{\text{theor}}(\alpha, \beta) = |\sin(\alpha B/\lambda) \cdot [\hat{B}_D(\alpha, \beta) \otimes G(\alpha, \beta)]|^2 \quad (2)$$

Where $\hat{B}_D(\alpha, \beta)$ is the complex amplitude generated by an individual sub-aperture and being back-projected onto the sky. For unobstructed pupils as in PERSEE, it is equal to $2J_1(\rho)/\rho$ where $\rho = \pi D/\lambda$, and J_1 is the Bessel function at the first order. $G(\alpha, \beta)$ is the fundamental mode of the exit filtering waveguide, after being projected back on-sky. It can be approximated by a gaussian function. Once we obtain the measured transfer function, we can compare it with the normalised theoretical one $\bar{T}^B_{\text{theor}}(\alpha, \beta) = N \cdot T^B_{\text{theor}}(\alpha, \beta)$, where $N = [\hat{B}_D(\alpha, \beta) \otimes G(\alpha, \beta)]^{-1}$ is the normalisation term.
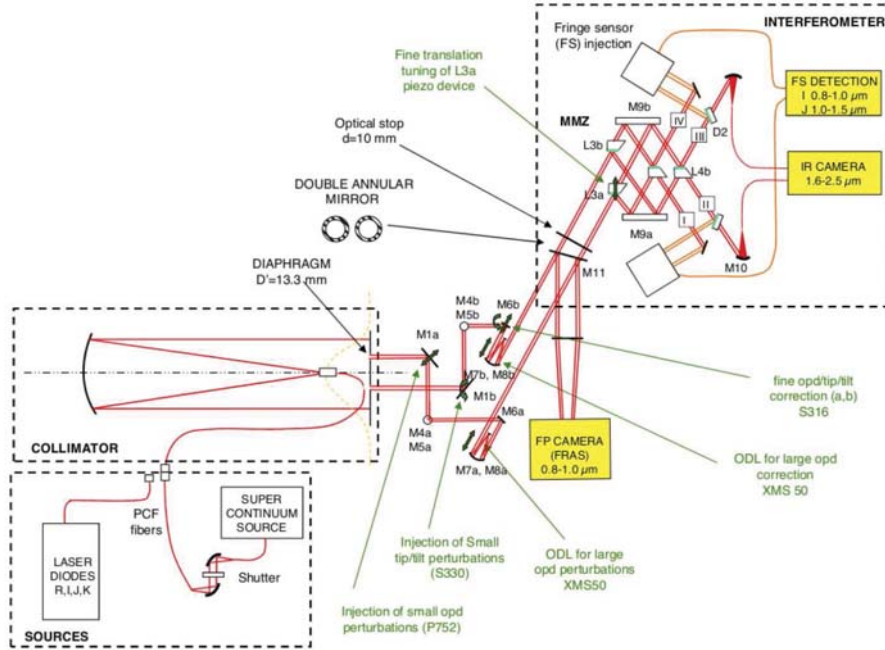
Figure 1.: *Layout scheme of the fibered nulling interferometer demonstrator PERSEE designed by Thales Alenia Space.*

3.   Results

We present preliminary results for the measure with internal tip-tilt from -36 to 36 arcseconds with a maximal OPD of 3.5 μm. The two apertures of PERSEE have a diameter of 13 mm and are separated by a baseline of 50 mm. It corresponds to a near-field off-axis on the order of $\simeq 1.4$ Airy disk radius and a ratio of baseline to diameter of pupils equal to $B/D = 3.2$ that gives ~ 7 fringes in an Airy disk region. For example, if we consider two apertures with a diameter of 10 cm the baseline is equal to 32 cm. Using Eq.1 we produced the map transfer function and its associated variance map shown for the channel $\lambda = 2.45$ μm respectively in Fig.2 and Fig.3. Fig.4 shows the theoretical transfer function obtained using Eq.2. The difference between measured and theoretical transfer function is shown in Fig.5. Both theoretical and subtracted maps are obtained for the channel $\lambda = 2.45$ μm. We see that the measured and modeled maps are fairly similar but with a difference that is larger than the standard deviation. The next step is to tune the model with a simple number of perturbation to obtain a good match with the measures. The value of the best null measured is on the order of magnitude of 10^{-4}. This value is considered deep enough to detect the zodiacal light with an accuracy of 1 zodi, comparable with the request for the PEGASE mission (Defrère et al. 2008). We hope that this null of 10^{-4} is sufficient for a comprehensive analysis of the statistic of the transfer function $\bar{T}_{\text{meas}}^{B}(\alpha, \beta)$. Note that the irregular region in the center of the left side of the measured transfer function has been caused by a sudden slight pressure change in the white room occurred during the measurements, due to the opening of the entrance door.
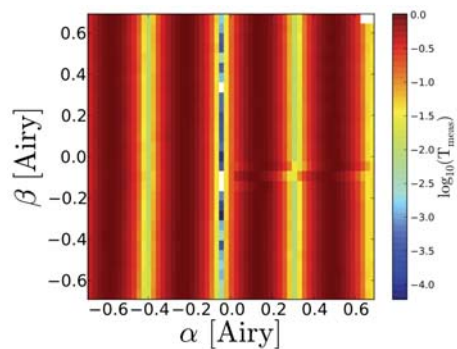
Figure 2.: *measured normalised transfer function* $\bar{T}^B_{\text{meas}}(\alpha, \beta)$ *for* $\lambda = 2.45$ μm.
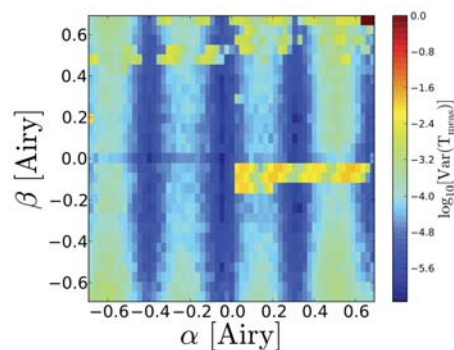

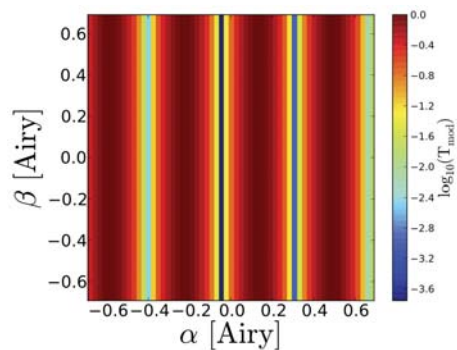Figure 3.: *variance of the measured normalised transfer function.*

Figure 4.: *theoretical normalised transfer function* $\bar{T}^B_{\text{theor}}(\alpha, \beta)$, *for* $\lambda = 2.45$ μm.
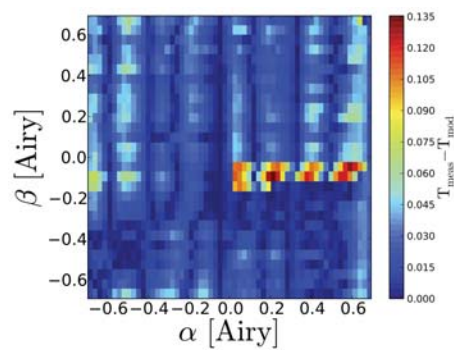

Figure 5.: *map of the subtraction between measured and theoretical transfer function.*

4.   Conclusions and perspectives

Using the PERSEE test bench, we collected data for a detailed characterisation of the polychromatic transfer function $\bar{T}_B(\alpha, \beta)$ for a realistic fibered nulling interferometer and study its statistics in time and space. We presented preliminary results obtained for the measure with the ratio $B/D = 3.23$. The value of the best null is on the order of 10^{-4}. If the transfer function is perfectly known, calibrated and stable, the performances of the model fitting or image reconstruction will be limited only by fundamental noises.

The precision and the stability of the transfer function for a nulling interferometer is the main limiting factor for the dynamic range that can be obtained for the investigated structures. Our goal is to analyse the variances and the covariances in time and between channels to evaluate the additional instrumental noise and hence the realistic limits of the approach. This is the starting point for a detailed characterisation of the nulling performances, especially for image reconstruction with an hyper-spectral approach and model fitting of very high-dynamic range scenes such as a star plus an exoplanet, or a star plus a debris disk with gaps.

[1] LESIA, Observatoire de Paris, 5 Place J. Janssen, 92195 Meudon, France, [2] CNES, 18 Av. E. Belin 31401 Toulouse Cedex 9, France, [3] ONERA, F-92322 Châtillon, France, [3] NASA Goddard Space Flight Center, Greenbelt, MD 20771, USA

References

Angel, J. R. P., & Woolf, N. J. 1997, ApJ, 475, 373

Bracewell, R. N., & MacPhie, R. H. 1979, Icarus, 38, 136

Danchi, W. C. et al. 2003, ApJ, 597, 57

Danchi, W. C. & Lopez, B. 2007, Comptes Rendus Physique, 8, 396

Defrère, D. et al. 2008, A&A, 490, 435

Hénault, F. et al. 2011, Proc. SPIE, 8151, 81510A

Jacquinod, S. et al. 2008, Proc. SPIE, 7013, 70131T

Lawson, P. R. et al. 2007, NASA STI/Recon Technical Report N, 8, 14326

Léger, A. et al. 1996a, Icarus, 123, 249

Léger, A. et al. 1996b, Ap&SS, 241, 135

Lozi, J. et al. 2013, American Astronomical Society Meeting, 221, 328.03

Ollivier, M. et al. 2009, Experimental Astronomy, 23, 403

Quirrenbach, A. 2001, ARA&A, 39, 353

Shao, M. et al. 1988, A&A, 193, 357

Tallon-Bosc, I. et al. 2007, New Astronomy Review, 51, 697

Thiébaut, E. 2009, New Astronomy Review, 53, 312